

A0005 **Mass Spectrometric Discrimination of Acyclic Stereoisomers via Competing Unimolecular Decompositions**

S0005 **1. Introduction**

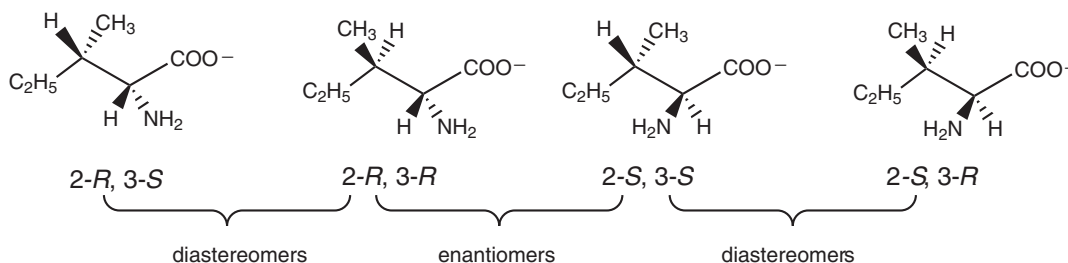
P0005 One of the most difficult challenges of structural analysis is to determine the relative stereochemistry of two asymmetrically substituted centers in an acyclic system. Mass spectrometry has long been known (although perhaps not widely recognized) to have the capacity to accomplish this. The subject has been reviewed, most recently a decade ago (<Bib1 Bib2 Bib3>1-3). In the intervening time, instrumentation and computational methods have made signal advances, which warrant not only an outline of newer developments but also a discussion of older work in light of current understanding.

P0010 This article focuses upon the problem of differentiating acyclic stereoisomers having two asymmetrically substituted tetrahedral centers, a category that embraces not only stereogenic carbon atoms, but also other elements, as well (see Chapter 4 (this volume): *Unimolecular Dissociation of Organic Ions: Reactions that Reveal Stereochemistry*). Consider a molecule with two asymmetric tetrahedral atoms. Each asymmetric center can have two absolute configurations, *R* or *S*. The molecule can therefore have four separable stereoisomers. The *R,R* and *S,S* isomers (nonsuperimposable mirror images of one another) will have identical spectroscopic properties

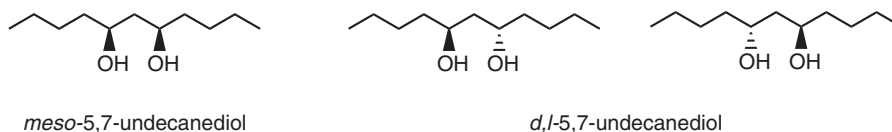
(except with regard to circularly polarized light), as will the *S,R* and *R,S* isomers. Nonsuperimposable mirror images are called 'enantiomers'. Stereoisomers that are not mirror images of one another (such as *R,R* and *R,S*) are called 'diastereomers' and will have different spectroscopic properties. Figure 1 illustrates these relationships for the carboxylate anions of the amino acid isoleucine.

The general theme, which will be presented here, is that diastereoselection in the unimolecular fragmentations of acyclic ions arises as a consequence of cyclic transition states. The placement of substituents in three dimensions imposes steric constraints on a ring, which can lead to different branching between competing pathways in one stereoisomer relative to another. Accordingly, this article is organized in terms of the size of the cyclic transition state(s) that have been discussed (in successive order: six-, five-, three-, and four-membered cyclic transition states). In some cases, isotopic labeling or theory justifies the inferred transition state; in others, the mechanism remains a subject of speculation.

It is possible for molecular symmetry to remove the chirality of a pair of enantiomers. For example, 5,7-undecanediol, illustrated in Fig. 2, possesses twofold molecular symmetry, such that the *S,R* and *R,S* configurations are superimposable. Therefore, this diol has only three stereoisomers, rather than four. The *S,R/R,S* isomer is achiral (since it has a plane of symmetry) and is called *meso*. The *R,R* and *S,S* isomers are sometimes called a *D,L* pair (or, if they are in a 50:50 mixture, the *rac* diastereomer).



F0005 **Figure 1**
Stereochemical relationships among the isomers of the isoleucine carboxylate anion. The 2-*R*, 3-*S* and 2-*S*, 3-*R* isomers are enantiomers of one another.



F0010 **Figure 2**
Stereochemistries of a molecule that can acquire a plane of symmetry.

P0025 Alternative strategies for differentiating acyclic stereoisomers have been treated elsewhere. For instance, the two diastereomeric carboxylate anions from isoleucine (Fig. 1) show different extents of dissociation via loss of CO plus water, but no variations are to be found among the competing fragmentation pathways themselves (<Bib4>4). Likewise, the *meso* and *rac* isomers of undecane-5,7-diol (Fig. 2) exhibit different extents of decomposition in their isobutane chemical ionization (CI) spectra (<Bib5>5). As has been reported so far, the MH^+ ions from both diastereomers yield the same proportions of fragment ions, but the extent to which intact MH^+ is observed differs markedly: in the *meso* MH^+ constitutes 46% of the ion current (at masses greater than those contributed by the CI reagent) while in the *rac* the MH^+ represents only 27%. This type of differentiation among diastereomers—relative degrees of dissociation of a parent ion—will not be further considered here. The discussion below confines itself to examples where the fragmentation patterns themselves display quantitative differences.

S0010 2. Six-Membered Cyclic Transition States

P0030 The pioneering work of Audier *et al.*, published in 1965, showed that the ratio of two competing fragmentation pathways can be used to distinguish acyclic diastereomers (<Bib6>6). In that work each example had two adjacent stereocenters, and the four possible isomers comprised two distinct pairs of nonsuperimposable mirror images (enantiomers). One set of enantiomers is often called the *threo* pair and the other the *erythro* pair. While two mirror image structures cannot manifest different chemical properties (in the absence of some additional chiral agent), a *threo* compound may exhibit features that differentiate it from its *erythro* isomer.

P0035 One way of representing the stereochemistry of two adjacent asymmetric, tetrahedral centers is to use Newman projections, as drawn in Scheme 1. A circle represents one asymmetric center, which stands in front of the other. The substituents on the two centers are drawn in a staggered arrangement. Although the structures in Scheme 1 depict single enantiomers, it is understood that (unless specifically stated otherwise) the molecules in question are racemic mixtures.

P0040 The differences between diastereomers, summarized by the tables in Scheme 1, are not large. The ratios of radical ions from H-transfer- m/z 56 from the vinyl compounds (Series 1) and m/z 106 from the phenyl compounds (Series 2)—to simple cleavage ions (M-55 from Series 1 and M-105 from the Series 2) from electron ionization (EI) show a subtle but significant change in going from *erythro* to *threo*. Such small differences (summarized by the ratio of ratios, r) can be measured reproducibly on a sector mass spectrometer, but would present a challenge for

many other types of instruments. A study of the effect of varying substituent R showed no systematic variation with steric bulk.

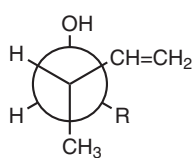
P0045 Péchiné explored an analogous competition in the hydrocarbon $CH_3CHPhCHPhCH_3$ and observed an even more subtle difference between the *meso* (analogous to *threo*) and the D,L (analogous to *erythro*) isomers (<Bib7>7). The r values for rearrangement (to give $[M-PhCH=CH_2]^+$) versus simple bond fission to give $Ph(CH_3)CH^+$ are close to unity.

P0050 Alvarez-Ibarra *et al.* (<Bib8>8) continued work along this line, investigating a series of diastereomeric alcohols in which an aryl group is directly attached to the carbinol carbon, as exemplified by Scheme 2. Here the r values were somewhat larger than in the series studied by Audier *et al.* (<Bib6>6). In Scheme 2, the ratio of simple cleavage (yielding an m/z 121 even-electron fragment) to the odd-electron $[M-H_2O]^+$ fragment (m/z 222) has a value significantly greater for the *threo* than for the *erythro*, giving a ratio of ratios $r = 1.29$ at 70 eV and $r = 1.35$ at 30 eV. This result can be rationalized in a variety of ways. The authors have considered elimination of water through six-membered transition states (for instance, via hydrogen transfer from the benzylic methyl to the oxygen, yielding a quinodimethide ion) versus five-membered transition states (via hydrogen transfer from the benzylic methylene). One might additionally suppose that *syn* elimination of water via a four-membered transition state could occur, setting the two aryl groups *cis* to one another in a newly formed double bond starting from the *threo* molecular ion and *trans* to one another starting from the *erythro*. To date, isotopic labeling studies that might distinguish among these options have not been reported.

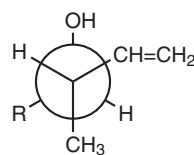
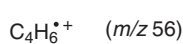
P0055 During 1968–1971, Green and coworkers demonstrated that mass spectrometry can distinguish deuterated diastereomers by means of rearrangements involving five- and six-membered cyclic transition states. In the fragmentation pattern of *threo* and *erythro* deuterated 2-chlorohexane, $CH_3CHClCH_2CH_2CHDCH_3$, for instance, they reported ion abundance ratios $[M-DCI]^{*+}/[M-HCl]^{*+}$ of 0.36 for the former and 0.26 for the latter (<Bib9>9, <Bib10>10). In this example, the two asymmetric centers are not adjacent, but are separated by two intervening methylene groups. Bringing the deuterium and chlorine atoms together requires a six-membered cyclic transition state. The ratio of ratios for the two diastereomers, $r = 1.4$, represents a significant increase over the values summarized in Scheme 1.

P0060 Green and coworkers also measured a comparable level of stereoselectivity in acetic acid elimination, $[M-DOOCCH_3]^{*+}$ versus $[M-HOOCCH_3]^{*+}$, from ionized *threo* and *erythro* $CH_3CH(O-COCH_3)CHDCH_3$ (*d*₁-*sec*-butyl acetate) (<Bib11>11, <Bib12>12, <Bib13>13), in which the stereocenters are

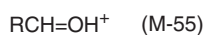
Series 1



erythro

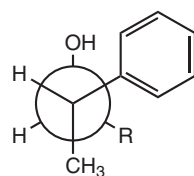


threo

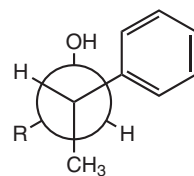
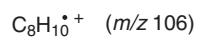


R	m/z 56 M-55		
	<i>erythro</i>	<i>threo</i>	<i>r</i>
CH_3	0.98	1.01	1.03
C_2H_5	1.28	1.32	1.03
$(CH_3)_2CH$	0.91	0.98	1.08
$(CH_3)_3C$	0.64	0.65	1.02

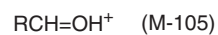
Series 2



erythro

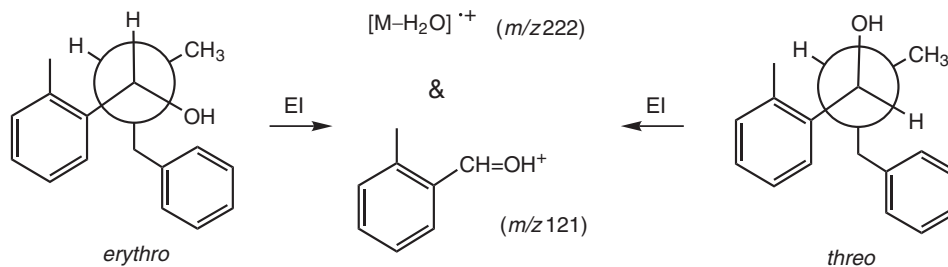


threo



R	m/z 106 M-105		
	<i>erythro</i>	<i>threo</i>	<i>r</i>
CH_3	3.33	3.71	1.11
C_2H_5	4.55	4.88	1.07
$(CH_3)_2CH$	4.00	4.44	1.11
$(CH_3)_3C$	3.18	3.28	1.03

F0030 *Scheme 1*



F0035 *Scheme 2*

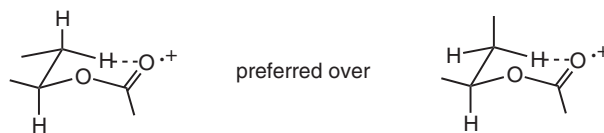
adjacent. This vicinal elimination also requires a six-membered cyclic transition state, as Scheme 3 illustrates for an unlabeled analog. Their subsequent examination of the energetic dependence (≤ 0.6 eV above threshold display stereoselectivity, which decreases with energy, but in more highly excited ions the selectivity fluctuates (though the average does not vary from what is observed in the ion source mass spectra). In any event, other decompositions compete with the stereoselective pathways, a complication that limits their utility for analytical purposes.

P0065 The production of odd-electron fragment ions from the deuterated *sec*-butyl acetates and from the alcohols summarized in Series 1 of Scheme 1 can be rationalized in terms of chair-like cyclic transition states, as illustrated in Schemes 3 and 4. The disposition of substituents in equatorial versus axial positions accounts for the observed preferences.

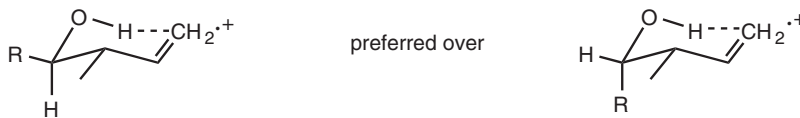
P0070 Similar types of transition states can be drawn for the deuterated 2-chlorohexanes and for Series 2 of Scheme 1 (referred to below simply as Series 2), but here the identities of the resulting odd-electron ions are by no means obvious. If internal hydrogen

transfer takes place via six-membered rings in the 2-chlorohexane molecular ion, the $[M-HCl]^{+\cdot}$ fragment should be distonic $C_6H_{12}^{+\cdot}$ (see Chapter 2 (this volume): *Structures and Properties of Gas-Phase Organic Ions: Ion-molecule Reactions of Distonic Radical Cations*; Volume 1, Chapter 9: *Organic Ion Chemistry (Positive): Distonic Radical Cations*) or else ionized dimethylcyclobutane, both of which are high energy structures relative to ionized hexenes. Likewise, a six-membered cyclic transition state for Series 2 implies that the m/z 106 ions should have the structure of ionized ethylidenecyclohexadiene, which is much less stable than its isomer, ionized ethylbenzene.

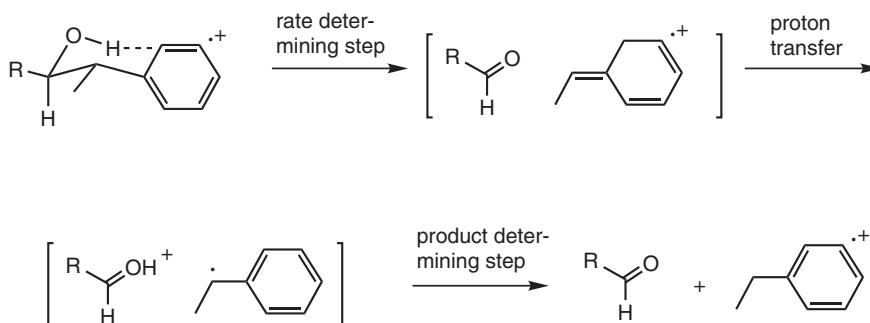
It is possible to speculate as to how the more stable ion might form. Scheme 5 illustrates such a pathway for Series 2 in terms of familiar mechanistic terminology. In the rate-determining step, the six-membered cyclic transition state leads to an ion-neutral complex (the species drawn in brackets) irreversibly (See Chapter 2 (this volume): *Structures and Properties of Gas-Phase Organic Ions: Theoretical Models for Ion-Neutral Complexes in Unimolecular Ion Decompositions*). This is the step that differenti-



F0040 Scheme 3



F0045 Scheme 4



F0050 Scheme 5

ates between diastereomers, but (as noted above) the resulting ion is a high energy species. Assuming that insufficient translational energy is imparted to the fragments for their complete separation, the charged and neutral fragments orbit about one another long enough for proton transfer to take place, forming a neutral benzylic radical in a second ion-neutral complex. Then, in the product determining step, the proton is returned to the radical to give the more stable radical ion, ionized ethylbenzene, the peak for which is observed in the mass spectrum.

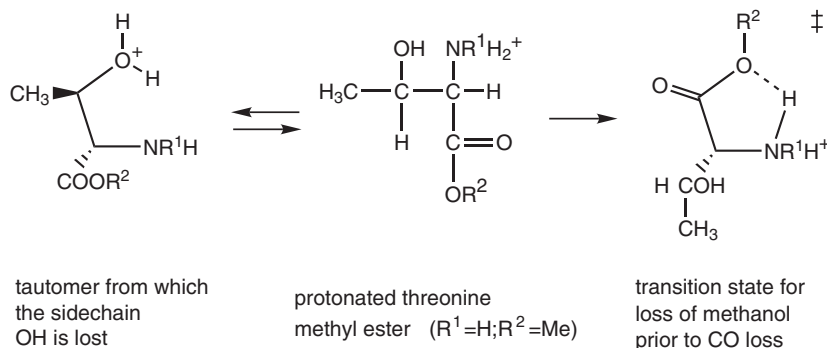
together requires a five-membered cyclic transition state in 2-chloropentane, it is tempting to surmise that, other things being equal, steric constraints exert themselves more dramatically in eliminations involving six-membered cyclic transition states.

When there is competition between a five-membered ring and another transition state, acyclic diastereoselection can result in pronounced effects, as in cationized amino acids. The fragmentation of protonated amino acid threonine (Scheme 6, $R^1=R^2=H$), its diastereomer (Scheme 7, $R^1=R^2=H$), and their methyl esters represent a case in point. The traditional designation for the diastereomers of these compounds is *threo* and *allo*. Collisionally activated dissociation (CAD; see Volume 1, Chapter 6: *Collisional Activation and Dissociation: Methodology*) of the MH^+ ions (<Bib14>14) displays two principal decomposition pathways: loss of water and carboxyl loss (loss of water and CO from the amino acid; loss of methanol and CO from the ester). A labeling study with ^{18}O shows that loss of a single water occurs from the side-chain oxygen (<Bib15>15). By contrast, both

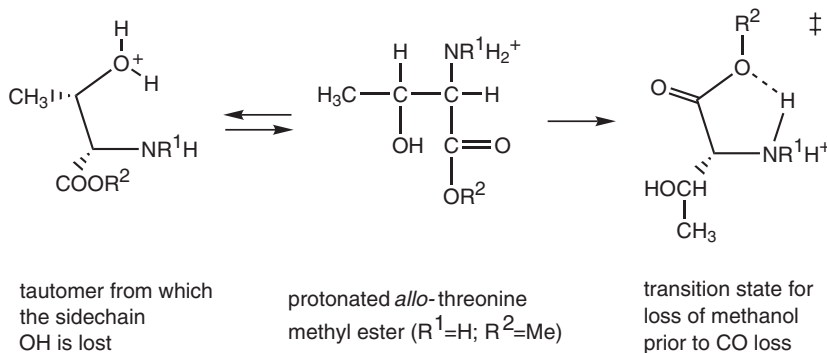
P0085

S0015 3. Five-Membered Cyclic Transition States

P0080 Green's initial demonstration of isotopic stereoselection (<Bib13>13) reported the elimination of HCl versus DCI from the diastereomers of deuterated 2-chloropentane, $CH_3CHClCH_2CHDCH_3$. In this original study, the ratio of ratios (using 9 eV electron ionization) had a modest value, $r=1.15\pm 0.015$, somewhat less than the value of r later observed for the deuterated 2-chlorohexanes discussed above. Since bringing the deuterium and chlorine atoms



F0055 Scheme 6



F0060 Scheme 7

carboxylic oxygens are lost when water and CO are expelled from the protonated amino acid.

P0090 The CAD of protonated *allo*-diastereomer shows a marked difference from that of protonated threonine, in that the loss of side-chain oxygen is much more prevalent ($\ll \text{Bib4} \gg 4$). The preferred tautomer for the $[M+1]$ ions has the proton on nitrogen. Transfer of the proton to one or the other of the OH groups is followed by water loss. Both transfers from nitrogen to oxygen occur by five-membered cyclic transition states, as Schemes 6 and 7 portray.

P0095 The same type of diastereomeric difference is seen in the methyl esters of the *threo* (Scheme 6, $R^1 = \text{H}$; $R^2 = \text{CH}_3$) and *allo* diastereomers (Scheme 7, $R^1 = \text{H}$; $R^2 = \text{CH}_3$), where side-chain water loss competes with loss of methanol and CO. To the left of Scheme 6 is drawn the minor tautomer from which the side-chain OH is lost. To the right is shown the transition state for forming the even less stable tautomer from which the carboxylic group is lost. Scheme 7 depicts the corresponding structures from *allo*-threonine. The final step in side-chain water loss involves formation of a three-membered ring, as will be described in the following section.

S0020 4. Three-Membered Cyclic Transition States

P0100 One of the best-known stereochemical preferences in organic chemistry comes from backside displacement in nucleophilic substitution at an sp^3 center. Internal backside attack has been inferred for elimination of a bromine atom from ionized 2,3-dibromobutane (but not for the corresponding dichloro compound) ($\ll \text{Bib16} \gg 16$). The 2,3-dihalobutanes can exist as two diastereomers. At low electron energies (12 eV), 99% of the total ionization (Σ) from the 2,3-dibromobutanes comes from three ions: the molecular ion ($\leq 5\% \Sigma$) and two even-electron fragment ions, $[M-\text{Br}]^+$ to $[M-\text{Br}-\text{HBr}]^+$. At higher energies, other fragment ions are formed, too, but even at 70 eV these two fragment ions dominate the mass spectrum (approximately 60% Σ).

P0105 Figure 3 plots the $[M-\text{Br}]^+$ to $[M-\text{Br}-\text{HBr}]^+$ abundance ratios for the two diastereomers. As is apparent, the *rac* isomer exhibits a greater fraction of $[M-\text{Br}]^+$ than does its *meso* diastereomer. While the abundances of the fragment ions vary with ionizing energy (as shown), the ratio of ratios r does not change significantly, but remains at a value near 1.1 (with the same value, $r = 1.14$, at 12 eV and at 70 eV). Also, the molecular ion abundance (not plotted) for the D,L is reproducibly higher than for the *meso*, with a ratio of $\% \Sigma$ values that remains constant at 1.6 over the entire energy domain studied.

P0110 The following explanation has been presented for the difference in molecular ion abundances. The *meso* leads to a *trans* orientation of the methyl groups when one bromine displaces another to form a cyclic

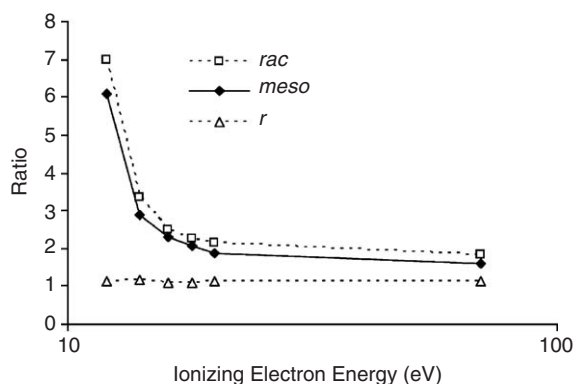


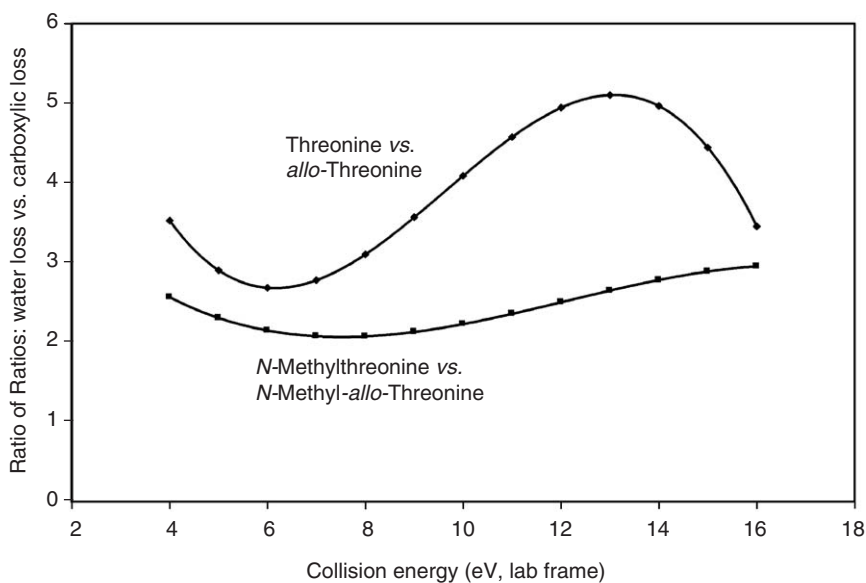
Figure 3

Ratios of $[M-\text{Br}]^+$ to $[M-\text{Br}-\text{HBr}]^+$ ions from *rac* (open squares) and *meso* (filled diamonds) from electron ionization of 2,3-dibromobutane, with the ratio of ratios r (open triangles) ($\ll \text{Bib15} \gg 15$).

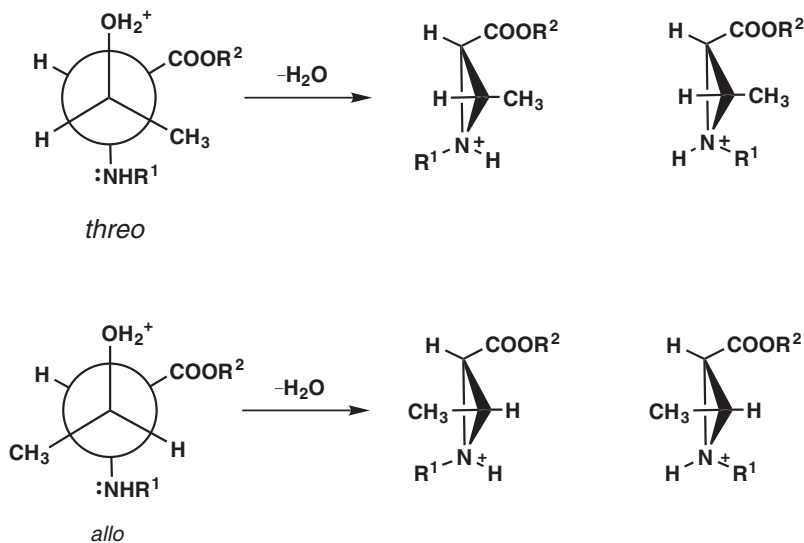
bromonium ion (the most stable structure for bromine-containing ions ($\ll \text{Bib17} \gg 17$)). By contrast the *rac* isomer must place the methyls *cis* to one another in the three-membered cyclic transition state. Hence, the *meso* exhibits a lower relative abundance of molecular ion.

The explanation for the differences in fragment ion abundances can be similarly rationalized. The order of fragmentation is presumed to be Br atom loss followed by HBr expulsion to form the $[M-\text{Br}-\text{HBr}]^+$ ions, which would be expected to have the allylic structure $\text{CH}_3\text{CH}=\text{CHCH}_2^+$ with delocalized positive charge. These allylic ions exhibit *cis-trans* isomerism, too. If HBr loss is assumed to occur via 1,2-*syn* elimination, the *meso*-dibromo precursor leads ultimately to a *trans* allylic cation and the *rac*-dibromo to a *cis* allylic cation. Hence, stereochemistry plays a role both in Br atom loss and in subsequent HBr expulsion. Since the *trans*-allylic cation is more stable than the *cis*, the *rac*-dibromo precursor should produce a lower $[M-\text{Br}-\text{HBr}]^+$ relative abundance than does the *meso*, as Fig. 3 summarizes.

Analogous stereochemical arguments account for the differences between the MS/MS spectra of the $M+1$ ions from the amino acid threonine and its diastereomer, *allo*-threonine. These two diastereomers are sometimes referred to simply as the *threo* and *allo* isomers. The r values are large for this stereodifferentiation, ranging from slightly less than 3 to slightly greater than 5, as the upper curve in Fig. 4 summarizes. As Schemes 6 and 7 imply, proton transfer takes place via five-membered cyclic transition states. Isotopic labeling implies that sidechain water is expelled in the course of forming three-membered rings ($\ll \text{Bib18} \gg \text{Bib19} \gg 18,19$), and the quantitative data have been interpreted to mean that



F0020 **Figure 4**
r values for collisionally activated decomposition (CAD) of protonated threonine versus protonated *allo*-threonine and of their *N*-methylated homologs.



F0065 **Scheme 8**

the large *r* values result from steric interactions in the transition states for the intramolecular backside displacements portrayed in Scheme 8. In addition, the CAD of the $\text{MH}^+ - \text{H}_2\text{O}$ ion from *allo*-threonine ($\text{R}_1 = \text{R}_2 = \text{H}$) is identical to that of protonated *trans*-3-methyl-aziridinecarboxylic acid.

N-methylation ($\text{R}_1 = \text{CH}_3$; $\text{R}_2 = \text{H}$) attenuates the value of *r*, as shown by the lower curve in Fig. 4 ($\ll \text{Bib4} \gg 4$). As Scheme 8 depicts, that outcome is consistent with an internal $\text{S}_{\text{N}}2$ as the rate-determining step for side-chain water loss: the *threo* isomer yields two aziridinium ions with very different steric

hindrances (one ion has three *cis* interactions; the other has one *cis* and two *trans*), while the *allo* isomer gives a pair ions that have, qualitatively, the same degree of steric hindrance (both have one *cis* and two *trans* interactions). Since there is not the large steric difference between *threo* and *allo* that is to be found in the unmethylated amino acids ($R_1 = R_2 = H$), the consequences of *N*-methylation provide a mechanistic test (<Bib4>4).

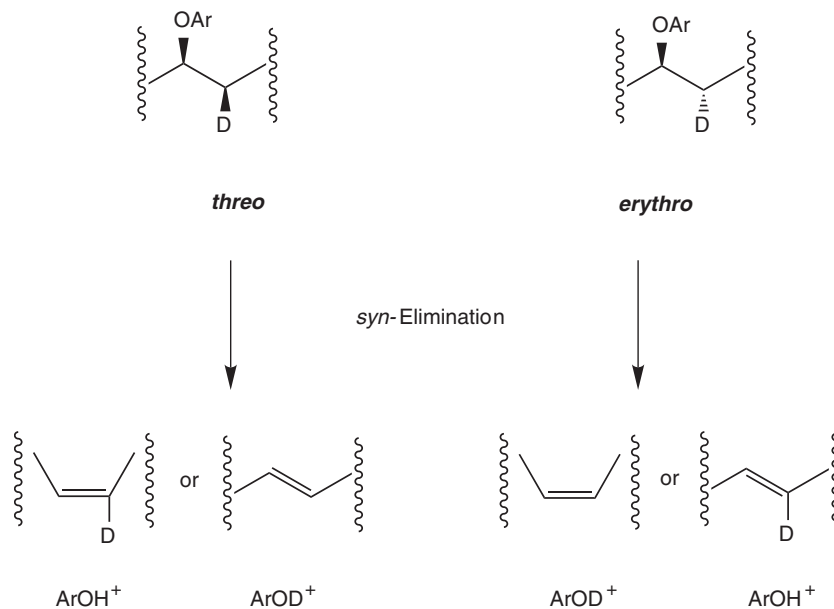
S0025 **5. Four-Membered Cyclic Transition States**

P0130 In 1988, Kondrat and Morton (<Bib20>20) reported stereoselectivity for alkene elimination from ionized $\text{CH}_3\text{CH}(\text{OPh})\text{CHDCH}_3$, for which the $[\text{C}_6\text{H}_5\text{DO}]^{+\bullet}/[\text{C}_6\text{H}_6\text{O}]^{+\bullet}$ fragment ratio has a value of 0.22 for *threo* and 0.16 for *erythro*. The ratio r of peak intensity ratios from electron ionization, in the range 1.3–1.4, remains virtually unchanged, regardless of whether the molecular ion decomposition is examined in the ion source mass spectrum, by CAD, or for metastable ions in the mass-resolved ion kinetic energy spectrum (MIKES, where alkene expulsion constitutes the only metastable ion decomposition) (see Volume 1, Chapter 3: *Instrumentation: Metastable Ions*). In 1991, Audier and Morton (<Bib21>21) used CAD to analyze the stereospecificity of a unimolecular gas phase reaction that produces ionized $\text{CH}_3\text{CH}(\text{OPh})\text{CHDCH}_3$ (See Volume 1, Chapter 6: *Collisional Activation and Dissociation: Via Ion-Neutral Complexes*).

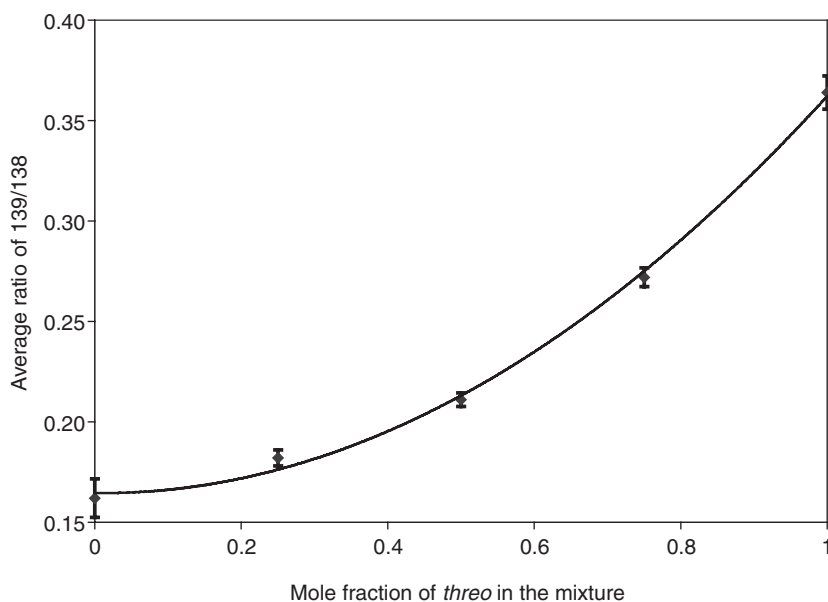
Labeling experiments (<Bib22 Bib23 Bib24 Bib25>22–25) demonstrate that alkene is expelled from ionized *sec*-alkyl ethers via *syn*-elimination, in which hydrogen moves from carbon to oxygen. The H/D competition thus reflects the choice between forming a *trans* double bond versus a *cis* double bond (see Scheme 9). Not only do radical cations ($\text{Ar} = \text{phenyl}$) give high r values (<Bib23 Bib24>23,24), but MH^+ ($\text{Ar} = \text{protonated } m\text{-dimethylaminophenyl}$) ions also display similarly large differences between diastereomers (as Fig. 5 summarizes) (<Bib25>25).

A number of experiments have shown that the alkene elimination from the radical cations proceeds via a four-center cyclic transition state and that the fragment ion has the structure of ionized phenol ($\text{PhOH}^{+\bullet}$) (<Bib19 Bib22 Bib23 Bib24>19,22–24). DFT calculations indicate that the transition state for elimination from even-electron ions is much the same as for odd-electron ions and that the remote electric charge in the MH^+ parent ions lowers the activation barrier by 10 kcal mol⁻¹ relative to *syn*-elimination from a neutral aryl ether (<Bib25>25). The compounds most closely examined have been the 3-hexyl aryl ethers, $\text{CH}_3\text{CH}_2\text{CH}(\text{OAr})\text{CHDCH}_2\text{CH}_3$, because they exhibit the largest ratio of $[\text{ArOD}]^+ / [\text{ArOH}]^+$ ratios yet observed, $r > 2$.

For all of the examples discussed here, hydrogen migration takes place prior to (or concomitant with) fragmentation. For isotopically labeled compounds H-transfer competes with D-transfer. To date, mass spectrometry has been used to analyze diastereomers only in cases where a stereospecific reaction gives one



F0070 **Scheme 9**



F0025 **Figure 5**
 Ratio of $m\text{-HOC}_6\text{H}_4\text{NHMe}_2^+$ to $m\text{-DOC}_6\text{H}_4\text{NHMe}_2^+$ fragment ions from electro-spray MS/MS of mixtures of *erythro* and *threo* $\text{CH}_3\text{CH}_2\text{CH}(\text{OAr})\text{CHDCH}_2\text{CH}_3$, where $\text{Ar} = m\text{-dimethylaminophenyl}$. The r value corresponds to the ratio for 100% *threo* (right hand side of the plot) divided by the ratio for 100% *erythro* (left hand side of the plot) ($\ll \text{Bib24} \gg 24$).

stereoisomer from one starting material and the opposite stereoisomer from another starting material. Published applications have looked at each starting material (and therefore each product) in independent experiments and have succeeded because the products turned out to be $>90\%$ diastereomerically pure. Given the possibility that two stereoisomers in a mixture will not decompose to equal extents, the ratio of ratios $r_{\text{threo}}/r_{\text{erythro}}$ has to be ≥ 1.3 in order to quantitate a sample in which *threo* and *erythro* are mixed together. Figure 5 summarizes results for mixtures of two diastereomers, where $r = 2.2$. For amino acids and their derivatives and for linear alkyl aryl ethers having the general formula $\text{CH}_3(\text{CH}_2)_m\text{CH}(\text{OAr})\text{CHD}(\text{CH}_2)_n\text{CH}_3$, the magnitude of the ratio of ratios r is suitable for mixture quantitation.

P0150 Since the analysis of deuterated diastereomers depends on abundance ratios of ions that are separated by 1 atomic mass unit, natural abundance ^{13}C interferes with measurement of the higher mass peak in an ordinary mass spectrum. Therefore, MS/MS techniques, which isolate ions containing only ^{12}C , need to be used, in order to give fragmentation patterns that are free from this interference. A calibration curve is shown in Fig. 5 ($\ll \text{Bib25} \gg 25$). There is a good prospect that mass spectrometry can

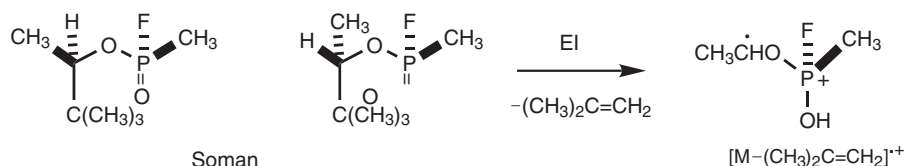
be used in the future to measure relative proportions of acyclic diastereomers in mixtures.

6. Outlook and Conclusions

S0030

P0155 Can one forecast the stereoisomers that ought to give different fragmentation patterns? Peptides represent the most prevalent group of acyclic compounds possessing more than one asymmetric center. It would be useful to have an *a priori* basis for deciding which should permit mass spectrometric discrimination. To date, differentiation of diastereomers has been reported only for dipeptides ($\ll \text{Bib26} \gg 26$), but future prospects are promising. The following general conclusion, drawn from the experimental examples presented above, may prove useful: competition between two alternative cyclic transition states gives higher r values than does competition between a cyclic transition state and a simple bond fission. The contrast between H/D selectivities versus the decompositions in Scheme 1 typifies this effect.

P0160 Can one forecast which stereoisomers ought not to give different fragmentation patterns? The emerging area of metabolomics raises this question with regard to small molecule mass spectrometry. Acyclic diastereomers are not always separable by gas chromatography. When they are, their GC/MS fragmentation patterns are sometimes indistinguishable. There may



Soman

 $[M-(CH_3)_2C=CH_2]^+$

 F0075 **Scheme 10**

be good reasons why this should be so. For instance, the nerve agent Soman, whose diastereomers are drawn in Scheme 10, possesses an asymmetric phosphorus as well as an asymmetric carbon. Electron ionization of Soman does not produce M^+ ions. The highest mass fragment in the reported mass spectrum comes from loss of isobutene, for which the distonic structure drawn to the right in Scheme 10 can be hypothesized. Most of the other fragment ions (e.g., subsequent loss of acetaldehyde) can be envisaged as descending from the $[M-(CH_3)_2C=CH_2]^{*+}$ ion (<Bib27>27). Since the expulsion of isobutene deletes the asymmetry of the stereogenic carbon, the distinction between diastereomers is lost, and their mass spectra are reported as being the same.

P0165 A long-term goal of mass spectrometry is to adduce chemical structure from a fragmentation pattern without the necessity of preparing an authentic sample. A logical first step in such an endeavor is, conversely, to predict fragmentation pattern from structure. The ability to do this from first-principles is not yet well developed. However, tools now exist, by which a mass spectroscopist can infer the pattern for one stereoisomer given the pattern for another.

 S0035 **Abbreviations**

P0170 **EI** Electron ionization
 P0175 **CAD** Collisionally activated dissociation
 P0180 **MIKES** Mass-resolved ion kinetic energy spectrum

Bibliography

- <Bib1>(1) Green, M. M. Mass Spectrometry and the Stereochemistry of Organic Molecules. *Topics in Stereochemistry* **1976**, *9*, 35–110.
 <Bib2>(2) Tureček, F. Stereochemistry of Organic Ions in the Gas Phase: A review. *Coll. Czech. Chem. Commun.* **1987**, *52*, 1928–1984.
 <Bib3>(3) Splitter, J. S. Stereochemical Effects in the Fragmentation Processes of Saturated and Unsaturated Acyclic Molecules. In: Tureček, F.; Splitter, J. S. (eds.) *Applications of Mass Spectrometry to Organic Stereochemistry*. VCH Publishers, 1994, pp. 83–102.

- <Bib4>(4) Serafin, S. V.; Zhang, K.; Aurelio, L.; Hughes, A.; Morton, T. H. Decomposition of Protonated Threonine, its Stereoisomers, and its Homologues in the Gas Phase: Evidence for Internal Backside Displacement. *Org. Lett.* **2004**, in press.
 <Bib5>(5) Wolfschütz, R.; Schwarz, H.; Blum, W.; Richter, W. J. Fragmentation of the Protonated Stereoisomers of 5,7-Decanediol and its Bis(trimethylsilyl) Ether Under Conditions of Isobutane Chemical Ionization. *Org. Mass Spectrom.* **1981**, *16*, 37–44.
 <Bib6>(6) Audier, H. E.; Felkin, H.; Fetizon, M.; Vetter, W. Effect of Stereoisomerism on Fragmentation in Mass Spectrometry. I. *Threo*- and *erythro*- β -Ethylenic and β -aromatic alcohols. *Bull. Soc. Chim. Fr.* **1965**, 3236–3238.
 <Bib7>(7) Péchiné, J. M. Diastereoisomer Pairs Studied by Mass Spectrometry. *Threo*- and *erythro*-2,3-diphenylbutane. *Org. Mass Spectrom.* **1972**, *6*, 805–814.
 <Bib8>(8) Alvarez-Ibarra, C.; Blanch, A.; Fernandez Gonzales, F.; Garcia Martinex, A.; Perez-Ossorio, R.; Plumet, J.; Quiroga, M. L. Comparative study of Diastereomers. I. Assigning *erythro-threo* Configurations to Acyclic Carbinols by Mass Spectrometry. *Anales de Quimica* **1975**, *71*, 723–729.
 <Bib9>(9) Green, M. M.; McGrew, J. G., II; Moldowan, J. M. Electron Impact-Induced 1,4-elimination. Barton Reaction in Disguise. *J. Am. Chem. Soc.* **1971**, *93*, 6700–6702.
 <Bib10>(10) Green, M. M.; Moldowan, J. M.; Hart, D. J.; Krakower, J. M. Dynamic Stereochemistry – A Comparator for Electron Impact and Pyrolytic Elimination of Acetic Acid from Acetates. *J. Am. Chem. Soc.* **1970**, *92*, 3491–3492.
 <Bib11>(11) Green, M. M.; Moldowan, J. M.; McGrew, J. G., II. Stereochemical Approach Toward the Structure of Gas-Phase Ions. *J. Org. Chem.* **1974**, *39*, 2166–2170.
 <Bib12>(12) Green, M. M.; McCluskey, R. J.; Vogt, J. A. Comparison Between the Stereoselective Thermal-Induced and Ionization-Induced Elimination of Acetic Acid from 2-Butyl Acetate. *J. Am. Chem. Soc.* **1982**, *104*, 2262–2269.
 <Bib13>(13) Green, M. M. Distinguishing Diastereotopic Hydrogens by Mass Spectrometry. A Direct Probe into the Transition State of an Electron-Impact-Induced Elimination Reaction. *J. Am. Chem. Soc.* **1968**, *90*, 3872–3873.
 <Bib14>(14) Kulik, W.; Heerma, W. A Study of the Positive and Negative Ion Fast Atom Bombardment Mass Spectra of Alpha-Amino Acids. *Biomed. Environ. Mass Spectrom.* **1988**, *15*, 419–427.
 <Bib15>(15) Van Dongen, W. D.; de Koster, C. G.; Heerma, W.; Haverkamp, J. The Diagnostic Value of the m/z 102 Peak in the Positive-Ion Fast-Atom Bombardment Mass Spectra of Peptides. *Rapid Commun. Mass Spectrom.* **1995**, *9*, 845–850.
 <Bib16>(16) Péchiné, J. M. Evidence for One Bromine Participation in the Expulsion of the other from 1,2-

AU:1

AU:2

Dibrominated Compounds. *Org. Mass Spectrom.* **1971**, *5*, 705–711.

<Bib17>(17) Vancik, H.; Percac, K.; Sunko, D.E. Isolation and the IR Spectra of Chloro- and Bromoethyl Cations in Cryogenic Antimony Pentafluoride Matrixes. *J. Chem. Soc. Chem. Commun.* **1991**, 807–809.

AU:3 <Bib18>(18) O'Hair, R. A. J.; Reid, G. E. *Rapid Commun. Mass Spectrom.* **1998**, *12*, 999–1002.

AU:4 <Bib19>(19) Reid, G. E.; Simpson, R. J.; O'Hair, R. A. J. *Am. Soc. Mass Spectrom.* **2000**, *11*, 1047–1060.

<Bib20>(20) Kondrat, R. W.; Morton, T. H. Stereochemical Differentiation in Decomposition of *Sec*-Butyl Phenyl Ether Molecular Ions. *Org. Mass Spectrom.* **1988**, *23*, 555–557.

<Bib21>(21) Audier, H. E.; Morton, T. H. Backside Displacement in the Unimolecular Gas Phase Decarboxylation of Alkyl Phenyl Carbonate Radical Cations. *J. Am. Chem. Soc.* **1991**, *113*, 9001–9003.

<Bib22>(22) Traeger, J. C.; Luna, A.; Tortajada, J. C.; Morton, T. H. Regio- and Stereochemistry of Alkene Expulsions from Ionized *sec*-Alkyl Phenyl Ethers. *J. Phys. Chem. A* **1999**, *103*, 2348–2358.

<Bib23>(23) Taphanel, M. H.; Morizur, J. P.; Leblanc, D.; Borchardt, D.; Morton, T. H. Stereochemical Analysis of Monodeuterated Isomers by GC/MS/MS. *Anal. Chem.* **1997**, *69*, 4191–4196.

<Bib24>(24) Morizur, J. P.; Taphanel, M. H.; Mayer, P. S.; Morton, T. H. Stereochemical Analysis of Deuterated Alkyl Chains by MS/MS. *J. Org. Chem.* **2000**, *65*, 381–387.

<Bib25>(25) Zhang, K.; Bouchonnet, S.; Serafin, S. V.; Morton, T. H. Stereochemical Analysis of Deuterated Alkyl Chains by Charge-Remote Fragmentations of Protonated Parent Ions. *Int. J. Mass Spectrom.* **2003**, *227*, 175–189.

<Bib26>(26) Tabet, J.-C.; Kagan, H. B.; Poulin, J.-C.; Meyer, D.; Fraisse, D. Differentiation of a Diastereoisomeric Dipeptide by Mass Spectrometry – Mass Spectrometry. *Spectrosc. Int. J.* **1985**, *4*, 81–90.

<Bib27>(27) Wils, E. R. J.; Hulst, A. G. Mass Spectra of some Pinacolyl-Containing Organophosphorus Compounds. *Org. Mass Spectrom.* **1986**, *21*, 763–765.

T.H. Morton
University of California, Riverside, CA, USA